FATIGUE CRACK PROPAGATION AND REMAINING LIFE ASSESSMENT OF SHIP STRUCTURES

Y. SUMI
Department of Naval Architecture and Ocean Engineering
Yokohama National University
Hodogaya-ku, Yokohama, Japan

ABSTRACT

The fitness for serviceability of structural members of ships, in which fatigue cracks could be found during in-service inspection, is investigated in order to prevent instantaneous failures of ships as well as the loss of serviceability such as oil and/or water tightness of critical compartments. The characteristics of fatigue crack propagation and the remaining life assessment of ship structures are discussed in the first part of the present paper, where the effects of weldment, complicated stress distributions including stress biaxialities at three-dimensional structural joints, structural redundancy, and crack curving are found to be of the primary importance. In the second part of the paper, discussions are made for an advanced numerical simulation method for the remaining life assessment, in which the effects of welding residual stresses, structural redundancy, and curved crack propagation are precisely taken into account. The simulated crack paths and the fatigue crack propagation lives are in fairly good agreement with the experimental results.

KEYWORDS

Ship structures, fatigue crack propagation, remaining life assessment, computer simulation, welding residual stress, structural redundancy, biaxial stress, crack curving

INTRODUCTION

Fatigue strength is one of the most important factors for the strength evaluation of ships, which generally consists of the strength assessment of buckling, plastic collapse, instantaneous fracture, and fatigue, because fatigue cracks are sometimes found at the discontinuities of ship structural details during in-service inspections after a certain period of service. In order to avoid the potentially hazardous situations, it is essential to assess the remaining crack propagation lives so that appropriate actions can be taken for the structural maintenance of ships. Although the conventional ship structural design is not based on the damage tolerant concept, these facts naturally lead to certain damage tolerance analysis of cracked components for the evaluation of the fitness for serviceability of a ship (Tomita *et al.*, 1994, Marine Board, 1995).

In the first part of the present paper, typical examples of fatigue cracks observed in ship structures are illustrated. Stress analyses of typical initiation sites of fatigue cracks in ship structures are discussed together with the simple estimates of stress intensity factors of small cracks. Then stress analyses of relatively long fatigue cracks in ship structures are categorized into several stages for the evaluation of the fitness for serviceability and also for the prevention of catastrophic failures. Various complicated stress analyses of fatigue cracks, which may be required for the assessment of crack propagation lives, are discussed including crack path predictions. It will be seen that various aspects of fatigue crack growth must be taken into consideration; i.e. spectrum

of loading, structural redundancy, welding residual stress, stress biaxiality, and non-collinear crack paths in order to investigate the structural integrity of ship structures.

In the second part of the paper, attentions are focused on a remaining life assessment of a complicated welded structure. The fatigue crack propagation law is modified to take into account the effect of welding residual stress. A step-by-step finite element approach is employed for fatigue crack path prediction, where a two-dimensional cracked domain is remeshed by the modified quadtree mesh generation algorithm, and the stress field ahead of the current crack tip is analyzed by taking account the higher order stress field parameters (Sumi, Chen, and Hayashi, 1995). A curved crack increment is determined by using the first order perturbation solution together with the local symmetry criterion. The crack tip is extended for a certain increment size, and the procedure is repeated for the next step. Furthermore, the effect of structural redundancy is precisely taken into account by the combination of the two-dimensional simulation system with a three-dimensional structural model through the superelement technique.

This method is applied to the simulation of fatigue crack propagation of welded test specimens. We measured the welding residual stress, some components of which showed a rather high compressive residual stress so that the reduction of effective stress intensity range could be expected. Numerical simulation has been carried out by using the superelement technique in order to idealize the whole welded structures. The simulated crack paths and the fatigue crack propagation lives are in fairly good agreement with the experimental results.

FATIGUE CRACK PROPAGATION IN SHIP STRUCTURES

Fatigue Cracks in Ship Structures

A typical example of the side structure of a crude oil carrier is shown in Fig. 1. Ships consist of outer skin plate such as side shell plates, deck plates, and bottom plates which are supported by internal longitudinal stiffeners and transverse girders as illustrated in the figure. Plate thicknesses of normal members are 10mm to 30mm, while ship length is 200m to 350m. Moreover, the ship structure has many structural discontinuities causing stress concentrations, most of which are the three-dimensional intersection of structural members connected by welding.

Fatigue cracks scarcely initiate at skin plates. They generally initiate at the weld toe of the intersection of longitudinal and transverse internal supporting members. Several kinds of cracks illustrated in Fig. 2 occurred in some crude oil carriers built in 1960's and 1970's. The majority of the cracks initiate around slots of the web of the transverse girder, where the longitudinal stiffener penetrates through the web. These fatigue cracks propagate in the transverse girders so that they hardly propagate to the shell plating. Investigations were made to reduce the stress concentration around the slots so that numbers of these fatigue cracks had been considerably reduced.

Figure 3 shows typical examples of a new type of fatigue cracks detected after three to four years of service at the side longitudinal stiffeners of comparatively new crude oil carriers built in mid 1980's (Mizukami *et al.*, 1994). In these ships high tensile steel of yield point over 315N/mm^2 is extensively used for the major parts of ship structures. Obviously these kind of cracks are potentially hazardous, because they propagate to the side shell plate and might cause oil leakage and oil pollution. Large numbers of cracks initiated at these internal structural members may be detected by in-service inspections, so that they could be repaired before reaching the shell plate.

Fatigue cracks in ship structures are typically initiated at weld toes of wrap-around weld and fillet weld, where stress concentrations due to structural discontinuity and weld geometry could be superimposed. Structural discontinuities can be uniquely defined by the detailed structural design, while the weld geometry depends largely upon workmanship of welding. This means that the quality control of the welding process is essential in order to avoid wide variations of peak stresses at the weld toe. Multiple initial cracks are usually formed along the weld toe in semi-elliptical shapes. If their initial distances are large compared with the thickness of the plate, they

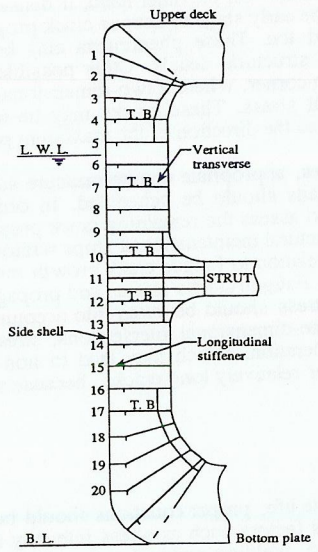

Fig.1 A side structure of a crude oil carrier.

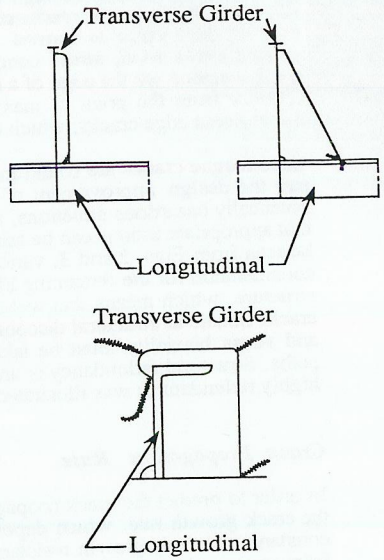

Fig.2 Fatigue cracks in transverse girders in 1970's.

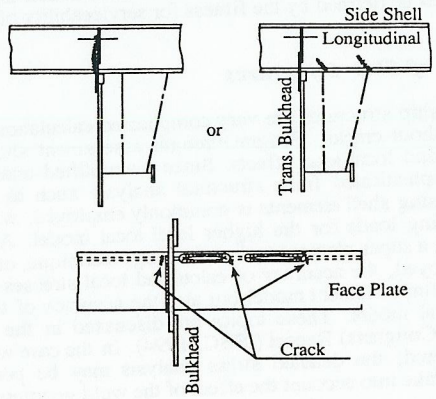

Fig.3 Fatigue cracks in longitudinal stiffeners in 1990's.

grow independently to through the thickness cracks. On the other hand, if dense initial cracks are formed, coalescence of cracks could occur at the early stage of fatigue crack propagation so that a surface edge crack is formed along the weld toe. These phenomena may be affected by an applied stress level, stress concentration, and structural details. Other possible sites of fatigue crack initiation are the edge of a hole or a sharp corner, where a two-dimensional edge crack may emanate from the point of maximum principal stress. These cracks may be modeled as two-dimensional edge cracks, which extend normal to the direction of the maximum principal stress.

Once fatigue cracks are found in ship structures, appropriate countermeasure such as the repair and the design improvement of structural details should be scheduled. In order to avoid the potentially hazardous situations, it is essential to assess the remaining crack propagation lives so that appropriate actions can be taken for the structural maintenance of ships without delay. As can be seen from Figs. 2 and 3, various factors in relation to fatigue crack growth must be taken into consideration for the remaining life assessment. Fatigue cracks initiate and propagate in a welded structure, which means that welding residual stress should be taken into account. Since fatigue cracks initiate at structural discontinuities of three-dimensional intersections, stress concentration and stress biaxiality must be taken into consideration, which may lead to non-collinear crack paths. Structural redundancy is another factor for relatively long cracks, because ship structure is highly redundant as was illustrated in Fig. 1.

Crack Propagation Rate

In order to predict the crack propagation or fatigue life, proper equations should be employed for the crack growth rate, which depends on various factors such as stress intensity range, material constants of crack growth resistance, stress ratio, welding residual stress, loading history and frequency, and environment. One of the commonly accepted expressions is Paris' equation. In this approach the effects other than the stress intensity range must be taken into account by choosing the material parameters appropriately for a specific condition. According to DnV classification note of mobile offshore units (DnV, 1984), the size of the initial crack should be considered in each case, taking account of experienced imperfection or defect sizes for various weldments, geometries, and inspection reliability. It is also suggested that a crack depth of 0.5mm (due to undercuts and microcracks at bottom of the undercuts) may be assumed for surface cracks starting from weld toe if no other information is available. The determination of final crack size must be defined by the fitness for serviceability of the members.

Stress Analysis of Ship Structures

Stress analyses of ship structures are very complicated calculations due to the complexity of ship structures even without cracks. Fatigue strength assessment should be based on local stresses induced by global and local load effects. Since a simplified analysis cannot give accurate local stresses, a very sophisticated finite structural analysis such as a multilevel hierarchical finite element modeling using shell elements is commonly employed, where a lower level global model is used for calculating loads for the higher level local model. An analysis of this kind can be carried our by using a super-element (substructuring) technique, or by using a zooming technique. If the latter is employed, the accuracy of calculated local stresses is governed not only by mesh density of the local finite element model but also the accuracy of the load and constraints applied to the local structural model. These topics are discussed in the ISSC (International Ship and Offshore Structures Congress) Report (ISSC, 1994). In the case where the crack propagation at a weld toe is considered, the detailed stress analysis may be performed by using solid finite elements which can take into account the effect of the weld geometry.

Simple Stress Intensity Estimates in Ship Structures

In order to calculate stress intensity factors, the local stresses calculated in an intact structure are decomposed into the membrane and bending components in the region where a crack is supposed

to propagate (WES2805, 1994). In order to calculate stress intensity factors, the membrane and bending components of the stresses are determined, and the stress intensity factors can be calculated by the following equation;

$$\Delta K_I=(\Delta\sigma_m \cdot F_m+\Delta\sigma_b \cdot F_b)\sqrt{\pi a}, \quad (1)$$

where a is the crack size, and F_m and F_b are the geometrical factors, which can be defined at the deepest point and the surface point, respectively, along a crack front line for three-dimensional surface cracks.

In order to calculate the stress intensity factors of surface cracks at weld toe, the detailed stress distribution in the neighborhood of the weld toe of an intact structure is determined first, so that the stress ranges $\Delta\sigma_m$ and $\Delta\sigma_b$ in Eq.(1) are obtained. Approximate stress intensity factors of surface cracks can be estimated by Eq.(1), in which formulas given by Raju-Newman (1981) are commonly used for F_m and F_b. Approximate formulas of stress intensity factors for various surface cracks and embedded elliptical cracks are found in a stress intensity handbook (Murakami, 1987, Carpinteri, 1994). An improved approach is proposed by Shiratori et. al. (1986), where Eq.(1) is modified so that not only the local membrane and bending components but also additional higher order components such as parabolic and cubic stress distributions are included in determining the stress intensity range. The method is applied to a life prediction of a surface crack initiated at wrap-around weld of ship structural details (Iino et al., 1992). Although the stress distributions of an intact structure is exactly determined for an actual structural details in the foregoing calculations, the stress intensity calculations are carried out based on the results of semi-elliptical surface crack in a flat plate. The effect of weld geometry is taken into account based on finite element crack analyses, and an approximate formula of a semi-elliptical crack at the toe of fillet weld has been proposed by Maddox et al. (1990). Further accumulation of numerical data based on finite element surface crack analyses may be required for an accurate determination of stress intensity factors at the toe of fillet weld and wrap-around weld.

Cracks emanating from a hole or a sharp corner can initially be modeled as an straight edge crack directed normal to the free surface. Internal through the thickness cracks initiated at stress concentrated region can be modeled as a two-dimensional internal crack in a plate. Stress intensity factors of through the thickness cracks are calculated by Eq.(1), where the geometric factors are found in a stress intensity handbook (Murakami, 1987).

Direct Stress Intensity Analyses in Ship Structures

Figure 4 illustrates a typical relatively long fatigue crack propagation in a ship structure, where it is categorized into the following five stages;

(i) surface crack propagation at the weld toe (see Fig. 5),
(ii) the propagation of a through the thickness crack in the flange (see Fig, 5),
(iii) curved propagation of a through the thickness crack in a web (see Fig. 6),
(iv) surface crack propagation at the normally intersecting skin plate (see Fig.7), and
(v) through the thickness crack propagation in a skin plate (see Fig.7).

In the first stage, a crack can be approximated by a semi-elliptical surface crack, which can in one way be modeled by three-dimensional solid finite elements with singular elements along the crack front, or in another way be modeled by shell elements with the use of line-spring elements. Although these kinds of crack modeling are incorporated in most general-purpose structural analysis codes, the finite element mesh generation, especially for the hexahedron solid elements, is the most time consuming part of the analysis. Once the surface crack penetrates through the thickness of the plate, the fatigue crack growth behavior becomes very complicated, because three crack tips appear at this stage, two in the flange and one in the web.

The crack path is essential for the third stage of the crack propagation. In some cases cracks propagate straightforward to the normally intersecting skin plate, while sharp crack curving could occur in other cases due to the stress biaxiality at the member intersection (see Fig.6). In these circumstances crack path prediction is required for the residual life prediction. Since a fully

automated simulation method of crack propagation combined with an appropriate crack path criterion has not been established for general three-dimensional plate structures, further research and development are expected in this area. Having propagated through the web, the crack may penetrates into the normally intersecting skin plate (see Fig. 7), whose shape is again modeled as a semi-elliptical surface crack. The stress intensity analyses can be performed in the same manner as those at the first stage. Up to this stage, the assessment of fatigue crack propagation life is important both for the residual life prediction and for the evaluation of loss of serviceability such as oil leakage and/or flooding of a certain ship compartment. The fifth stage is essential for the prevention of the catastrophic failure of a whole ship structure. Once cracks of this kind are found, extensive inspections must be carried out along the similar locations of periodical structures in order to examine the possibilities of the formation of multiple site cracks which may significantly reduce the fatigue crack propagation life (Sumi *et al.*, 1996).

ADVANCED SIMULATION METHOD FOR REMAINING LIFE ASSESSMENT OF WELDED STRUCTURES

In the previous section the calculation procedures of stress intensity factors in ship structures have been discussed, where approximate formulas of stress intensity factors may be applied to relatively short cracks. If the crack extends further, the elastic interaction between the adjacent structures must be taken into account. Also the extending cracks could be loaded under biaxial stress conditions at the intersection of structural members, which may lead to curved crack propagation. In the second part of the paper, discussions are made for the recently developed simulation method, which may give an accurate assessment of both the crack propagation life and the final failure mode of a welded ship structure.

A step-by step finite element approach, which was originally developed for brittle crack paths (Sumi, 1990), has been modified to fatigue crack path prediction (Sumi, Chen, and Hayashi , 1995, Sumi, Chen, and Wang, 1995), where an accurate stress intensity analysis, a proper crack path criterion, an accurate growth rate equation, and an automatic mesh generation algorithm are required. A fatigue crack is modeled as a two-dimensional crack in a plate, and the simulation procedure is shown in Fig. 8. In each step a cracked domain is subdivided into new finite element mesh by a modified quadtree method (Yerry and Shephard, 1983), and the stress field parameters including stress intensity factors are determined by the method of superposition of analytical and finite element solutions (Yamamoto and Tokuda, 1973). Then the crack tip is moved to a certain point on the predicted path, which is obtained by using the first order perturbation solution (Sumi, Nemat-Nasser, and Keer, 1983) with the local symmetry criterion (Kitagawa *et al.*, 1981). The crack growth life is evaluated, and the procedure will be repeated until the final stage of the crack propagation is reached.

In this paper, the above step-by-step approach is extended to include the superelements, which represent the complicated three-dimensional welded structures surrounding a cracked zone. A relatively relaxed connecting method has been introduced by using the generalized inverse matrix of a nodal transformation matrix so that the nodal points of the crack propagating domain and those of the superelements may locate at different points along the interface boundary without loss of solution accuracy. Comparing the present superelement method with the so-called zooming technique using displacement boundary conditions, it has been confirmed that more reliable results are expected by the present method.

SIMULATION AND EXPERIMENTS ON FATIGUE CRACK PROPAGATION IN WELDED SPECIMENS

Testing Conditions

Fatigue crack propagation tests are carried out, where the geometry and the loading condition of the test specimens and the notch details are illustrated in Fig. 9. Various biaxial stress range ratios,

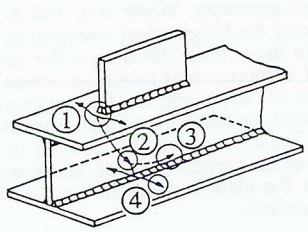

Fig.4 Typical fatigue crack propagation in a ship structure.

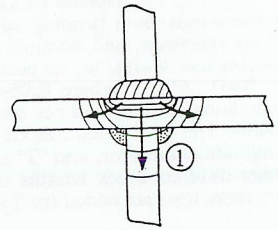

Fig.5 A surface crack propagation from weld toe to flange and web plates.

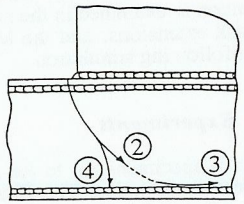

Fig.6 Fatigue crack propagation in a web plate.

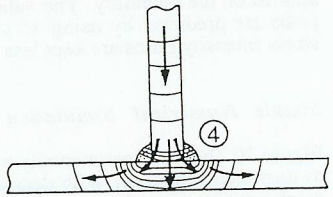

Fig.7 Fatigue crack propagation from web to skin plate.

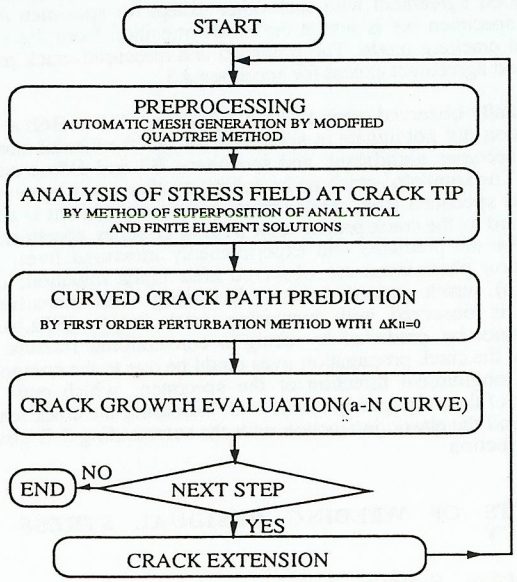

Fig.8 Flowchart of the Simulation

$r=\Delta\sigma_2/\Delta\sigma_1$, are attained by changing the specimen geometry, where $\Delta\sigma_1$ and $\Delta\sigma_2$ represent the nominal maximum bending stress range acting along the longitudinal direction at the upper edge of the specimen, and nominal axial stress acting in the vertical direction at the central part of the specimen of width, w, respectively. The repeated minimum and maximum stress ratios is given by $R=P_{min}/P_{max}$, where $0.05<R<0.07$ in the present experiments. The geometry and loading conditions of all specimens are listed in Table 1, and the material is ship structural steel of class KA36. The final failure mode is also shown in Table 1, where "L" denotes the failure of the longitudinal member, and "T" indicates the failure of the vertical member. Since we often observe rather different crack lengths on the both sides of the plate surfaces in the B-series specimens, two more tests are added for Types B5 and B6 specimens.

In this section we first consider the simple case, where the simulation is carried out disregarding both the elastic interaction and the welding residual stresses. A two-dimensional zoomed up domain is selected, and its boundary conditions are prescribed in such a way that the displacement calculated by the three-dimensional finite element analysis of the intact whole specimens are applied on the boundary. The validity of this simplification is examined in the next section. Crack paths are predicted by using 15 to 20 incremental crack extensions, and the Mode II to Mode I stress intensity ratios are kept less than 5 percent in the following simulation.

Simple Numerical Simulation Compared with Experiments

Figure 10 shows experimentally measured crack paths of specimens A1 to A6. The cracks tend to turn their directions with decreasing the biaxial stress range ratios. The final direction of the crack propagation of specimen A1 is nearly perpendicular to the initial direction. Although the biaxial stress range ratios of specimens A3 and A4 are similar, the observed paths are rather different. This indicates that the final mode of failure is governed not only by the biaxial stress range ratios but also by the sizes and shapes of the stress concentrated regions. Simulated crack paths of A-series specimens are also illustrated in Fig. 10. Simulated and measured crack paths are in fairly good agreement with each other except for specimen A3. It seems that the loading condition for specimen A3 is just at the mode transition from the straight cracking mode to the sharply curved cracking mode. The predicted and measured crack propagation lives are found to be in fairly good agreement except for specimen A3.

The experimentally observed crack paths of specimens B1 to B6b are shown in Fig. 11. Fatigue crack propagation did not initiate in specimen B4. As the biaxial stress range ratio increases, the crack turning becomes significant, and specimens B3 and B5a,b and B6b failed after complete crack turning. The simulated crack paths exhibit a rather good agreement with the measured crack paths except for specimen B6a, whose crack path in experiment is almost straight after the initial kink. With regard to the crack propagation lives of B-series specimens, rather large discrepancies are observed for the predicted and experimentally measured lives. In the experiments various crack propagation phenomena are observed after crack initiation; i.e. crack growth is almost arrested (B6a,b), crack growth rate is decreasing with increasing crack length (B3), and stationary rate is observed with increasing crack length (B5a,b). It is obvious that these phenomena cannot be predicted by using a conventional fracture mechanics approach. The discrepancies of the crack propagation lives could be due to the compressive welding stress acting parallel to the longitudinal direction of the specimen, which may reduce the effective stress intensity ranges of the propagating cracks with increasing the crack length. The effects of welding residual stress and the elastic interaction with the surrounding 3-D structures will be discussed in the subsequent section.

THE EFFECTS OF WELDING RESIDUAL STRESS AND STRUCTURAL REDUNDANCY

Effects of Welding Residual Stress

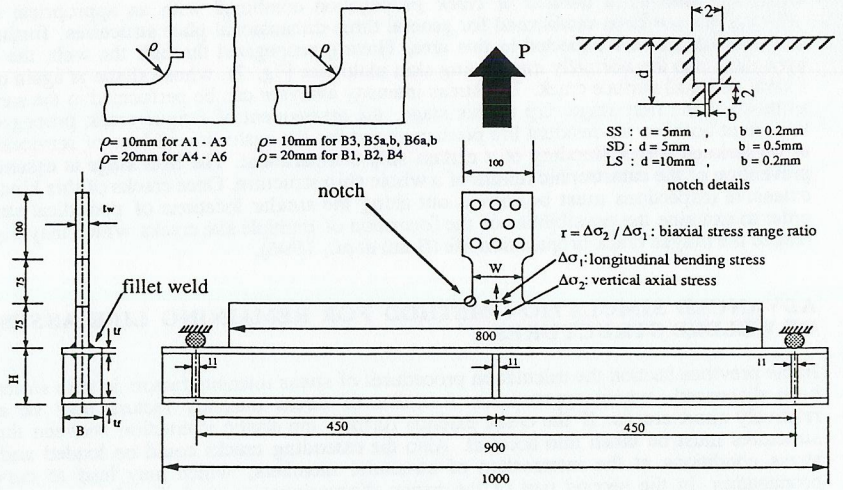

Fig.9 Geometry and loading condition of the specimen.

Table 1 Geometry, loading condition, and some test results of the specimens.

Specimen	H(mm)	B(mm)	t_w(mm)	t_f(mm)	W(mm)	r	Notch	P_{min}(kN)	P_{max}(kN)	Path	Mode
A1	60	50	15	11	75	0.21	SS	4.9	69	curved	L
A2	85	50	15	11	75	0.296	SS	4.9	78	curved	L
A3	130	50	15	11	75	0.490	SS	4.9	88	curved	L
A4	105	160	15	15	75	0.6	SD	5.9	88	straight	T
A5	135	160	15	20	75	1.0	SD	5.9	88	straight	T
A6	175	160	15	20	75	1.5	SD	5.9	88	straight	T
B1	105	160	15	15	75	0.6	SD	2.0	78	curved	L
B2	135	160	15	20	75	1.0	LS	5.9	93	curved	L
B3	105	160	11	15	55	1.02	SS	4.9	88	curved	T
RB3	(for residual stress measurement)										
B4	175	160	15	20	75	1.5	LS	5.9	93	no propagation	
B5a	135	160	11	15	55	1.51	SS	4.9	88	curved	T
B5b	(same as the above)							4.9	97	curved	T
RB5	(for residual stress measurement)										
B6a	160	160	11	15	55	1.96	SS	4.9	88	kinked	–
B6b	(same as the above)							4.9	97	curved	T
RB6	(for residual stress measurement)										

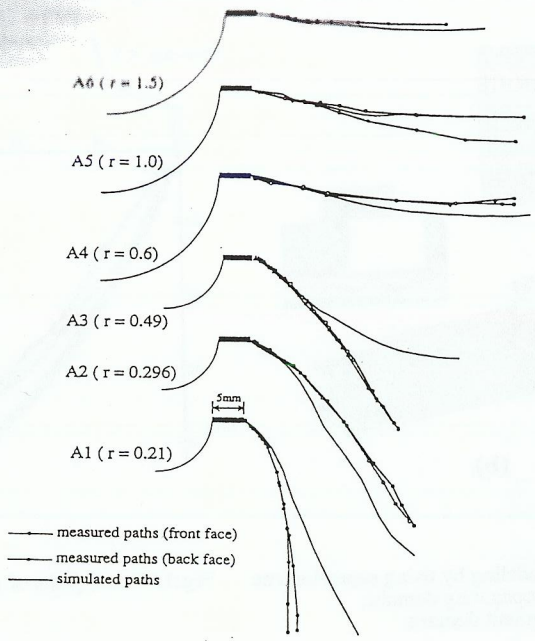

Fig.10 Measured and simulated paths of A-series specimens.

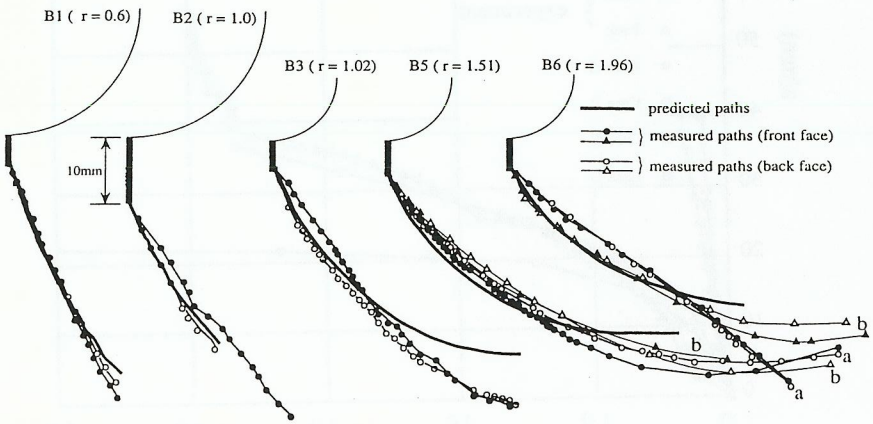

Fig.11 Measured and simulated paths of B-series specimens.

Since the very slow crack propagation in comparison with the simulated results is observed in experiments, especially in B-series specimens, welding residual stress measurements were carried out for specimens RB3, RB5, and RB6, which were the analogs of the fatigue test specimens B3, B5a,b and B6a,b, respectively. The geometry of the specimens prepared for residual stress measurement is shown in Fig.12. The residual stress measurement is carried out by the conventional sectioning technique using biaxial electric-resistance strain gages along the two sections; the one is the mid-span section (a-section) and the other is b-section, where the initial machined notches are made in the fatigue test specimens. The measured longitudinal residual stresses are shown in Fig. 13, which shows very high compressive stress distribution. The maximum compressive residual stress is between -200MPa and -300MPa, which is attained approximately 30mm from the top edge of the specimens. It should be noted that the measured value of residual stress is the average stress in the thickness direction. It is also found that the normal stress acting in the vertical direction is very small so that it can be disregarded in the following discussions.

How does the residual stress affect on fatigue crack propagation? Since the residual stress is a stationary stress, we assume that it simply changes the stress ratio, R. For a given cracked geometry we can calculate the stress intensity factor contributed purely from the residual stress. Let us denote the opening mode of stress intensity factors due to the applied load and the residual stress by K_I and K_{IR}, respectively. In the following analysis, we assume that the ranges of the stress field parameters at the crack tip are accounted for as far as, $K_I + K_{IR} > 0$, holds during a load cycle. It should be noted that the stress intensity factor, K_{IR}, always takes negative value due to the compressive residual stress in the following analysis. For crack propagation calculation, we shall use the Paris' constants for class KA36 steel.

Simulation Including the Effects of Structural Redundancy

Since rather different crack lengths are sometimes observed on the front and back surfaces of the several B-series specimens, we shall investigate the crack growth behavior of specimen B3 in detail which shows almost the same crack propagation rates on the both sides of the specimen surface. Numerical simulation has been carried out for the following four cases;

(Case A): zooming analysis disregarding the effect of welding residual stress,
(Case B): zooming analysis including the effect of welding residual stress,
(Case C): superelement analysis disregarding the effect of welding residual stress,
(Case D): superelement analysis including the effect of welding residual stress.

In Cases C and D the superelement technique is used in order to idealize the structural redundancy of the whole welded specimen, whose finite element model is illustrated in Fig. 14. In Cases A and B the zoomed up region is 100mm in length and 60mm in width, which is slightly different from the model used to obtain the result illustrated in Fig.11.

The simulated crack paths are compared with experimental results in Fig. 15, in which they show a rather good agreement with each other. On the contrary, the crack propagation lives show significant discrepancies (see Fig. 16). If we disregard the effects of the compressive welding residual stress, the predicted crack propagation lives are considerably shorter than the experimental results (Cases A and C), while the crack growth is arrested in Case B due to the excessive displacement constraint at the zooming boundary. As is shown in the figure, Case D, which precisely takes into account both the welding residual stress and the structural redundancy, shows an excellent result.

CONCLUSIONS

Fatigue crack propagation in ship structures and the remaining life assessment are reviewed in the first part of the present paper. Fatigue crack propagation in ship structures are categorized for the evaluation of the fitness for serviceability and also for the prevention of catastrophic failures. In the second part of the paper, an advanced simulation method is introduced for the remaining life assessment, in which the effects of welding residual stresses, structural redundancy, and curved

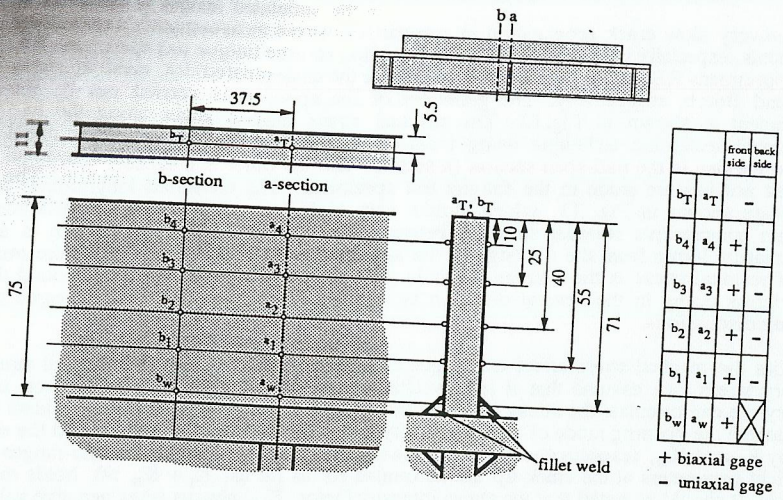

Fig.12 The arrangement of strain gages for residual stress measurement.

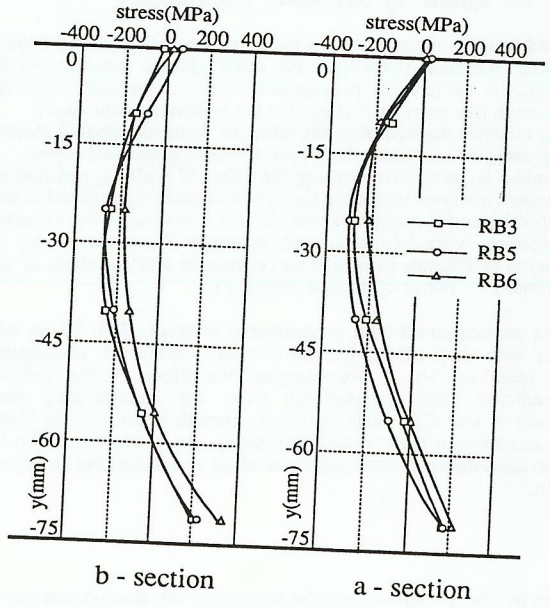

Fig.13 Residual stress distribution along a-section and b-section.

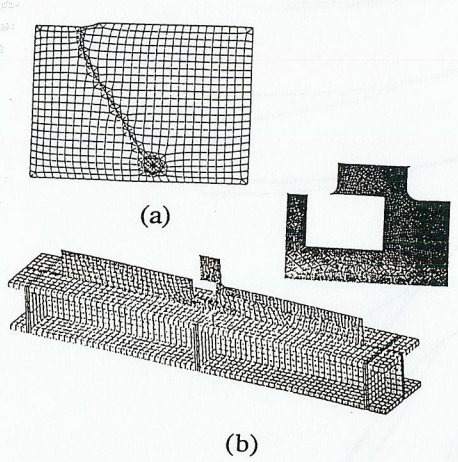

Fig.14 Structural modeling by using superelement:
(a) crack propagating domain;
(b) superelement domain.

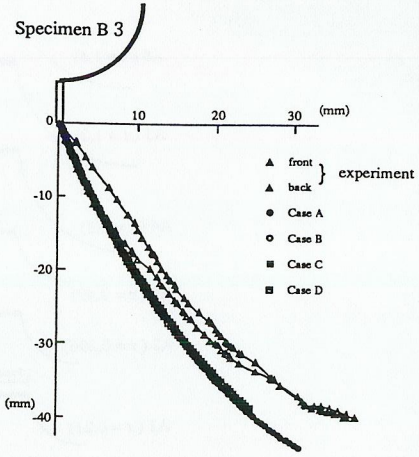

Fig.15 Crack paths of specimen B3.

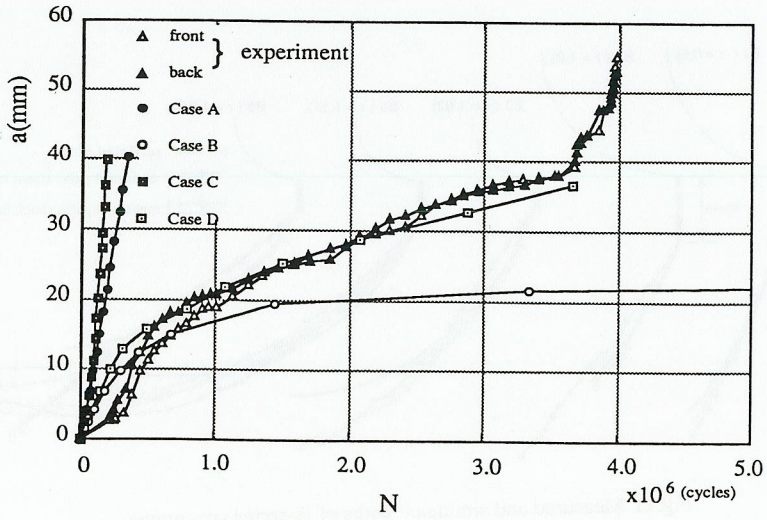

Fig.16 Measured and simulated crack propagation lives of specimen B3.

crack propagation due to stress biaxiality are taken into consideration. By using the proposed superelement technique and the crack propagation model, these factors are precisely taken into account so that the simulated crack paths and the fatigue crack propagation lives are found to be in good agreement with the experimental results.

ACKNOWLEDGMENT

This work has been supported by Grant-in-Aid for Scientific Research (B-04555098 and A-08305037) from the Ministry of Education, Science and Culture and by the research projects SR216 and SR219 of Shipbuilding Research Association of Japan.

REFERENCES

Amestoy, M. and J. B. Leblond (1992). Crack paths in planar situations-II Detailed form of the expansion of the stress intensity factors, Int. J. Solids Structures 29-4, 465-501.

Det norske Veritas (1984). Fatigue strength analysis for mobile offshore units, In: *Classification Note No.30.2*, Høvik, Norway.

Iino, N., O. Ushirokawa, I. Neki, H. Sasajima, and Y. Nakajima (1992). Study on fatigue strength of 50HT steel with wrap-around weld, J. Soc. Naval Arch. Japan 171, 437-448 (in Japanese).

ISSC (1994). Committee II.1 Report: Quasi-static load effects, In: *Proceedings of the 12th International Ship and Offshore Structures Congress, Vol.1*, St. John's, Canada 151-231.

Kitagawa, H., R. Yuuki, and K. Tohgo (1981). Fatigue crack growth under combined modes of stress intensity factors, J. JSME A47-424, 1283-1292 (in Japanese).

Marine Board (1995). Symposium and workshop on the prevention of fracture in ship structures, National Academy of Sciences, Washington, D.C.

Maddox, S. J. and R. M. Andrews (1990). Stress intensity factors for weld toe cracks, presented at Localised Damage 90, June 26-28, 1990, Portsmouth, U.K.

Mizukami, T., I. Ishikawa, and M. Yuasa (1994). Trends of recent hull damage and countermeasures, ClassNK Technical Bulletin 12, 25-45.

Murakami, Y. (ed.) (1987). Stress intensity factors handbook, Vols. 1-2, Pergamon Press.

Newman, J. C., Jr. and I. S. Raju (1981). Stress intensity factor equations for cracks in three-dimensional finite bodies, NASA Technical Memorandum 83200, 1-49.

Shiratori, M., T. Miyoshi, and K. Tanikawa (1986). Analysis of stress intensity factors for surface cracks subjected to arbitrarily distributed surface stresses, Trans. JSME A52-474, 390-398 (in Japanese).

Sumi, Y., S. Nemat-Nasser, and L. M. Keer (1983). On crack branching and curving in a finite body, Int. J. Fracture 21, 67-79; (1984) Erratum, Int. J. Fracture 24, 159.

Sumi, Y. (1990). Computational crack path prediction for brittle fracture in welding residual stress fields, Int. J. Fracture, 189-207.

Sumi, Y., Y. Chen, and S. Hayashi (1995). Morphological aspects of fatigue crack propagation, Part-I Computational procedure, (submitted for publication).

Sumi, Y., Y. Chen, and Z.N. Wang (1995). Morphological aspects of fatigue crack propagation, Part-II Effects of stress biaxiality and welding residual stress, (submitted for publication).

Sumi, Y., Z. Bozic, H. Iyama, and Y. Kawamura (1996). Multiple fatigue cracks propagating in a stiffened panel, J. Soc. Naval Arch. Japan 179, 407-412.

Tomita, Y., M. Toyosada, Y. Sumi, and A. Kumano (1994). Fatigue crack propagation in ship structures, In: *Handbook of Fatigue Crack Propagation in Metallic Structures* (A. Carpinteri, ed.), Vol. 2, Chap 44, 1609-1642, Elsevier, Amsterdam.

WES 2805 (1994). Method of assessment of defects in fusion welded joints with respect to instantaneous failure, The Japan Welding Engineering Society.

Yamamoto, Y. and N. Tokuda (1973). Determination of stress intensity factors in cracked plates by the finite element method, Int. J. Numer. Meth. Engng. 6, 427-439.

Yerry, M.A. and M.S. Shephard (1983). A modified quad-tree approach to finite element generation", IEEE Computer Graphics and Applications Jan./Feb., 39-46.